The nodal section method for the analysis of box girders

The Nodal Section Method for the Analysis of Box Girders

La méthode de section nodale pour l'analyse de poutres en caisson

Die nodale Querschnitts-Methode zur Berechnung von Kastenträgern.

K.C. ROCKEY
Professor and Head of Department, Department of Civil and Structural Engineering, University College, Cardiff.

H.R. EVANS
Lecturer, Department of Civil and Structural Engineering, University College, Cardiff.

1. Introduction

The Nodal Section Method has been developed to provide a relatively simple method of analysis for both single-span and continuous box girders in which the geometry of the cross-section varies along the length of the girder. Although the method assumes a simplified structural behaviour in order to reduce the amount of computation required, it does in fact provide results of a high degree of accuracy. It is anticipated that, since the amount of computation involved is relatively small, the method will prove to be useful during the design of a box girder, when several analyses may be necessary in order to investigate the effect of changing various dimensions. In such a situation, the use of the Finite Element Method which involves extensive calculations proves to be prohibitively expensive.

The Nodal Section Method is based on a method of analysis previously applied to folded plate structures. Indeed, a box girder is only a particular type of folded plate structure, in which the plates have been arranged so as to form a closed section, as shown in Fig. 1. In recent years much research has been devoted to the analysis of folded plates and two main methods have been established, these being the "Elasticity Method" [1, 2] and the "Ordinary Method" [3, 4].

Of these two methods, the Elasticity Method is the more accurate and this method has, in fact, already been adapted to box girder analysis by SCORDELIS [5, 6], this method being termed the "Folded Plate Method". In this method, each component plate of the box girder is considered as an individual element and a stiffness matrix derived for it, the individual stiffness matrices for the plates then being assembled together as in a matrix stiffness method of analysis. The bending of each plate element normal to its plane is analysed by plate flexure theory, and its in-plane bending is analysed by plane stress theory.

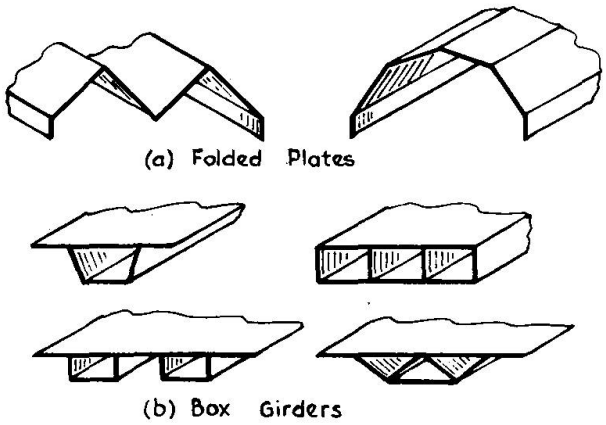

Fig. 1. Typical folded plate and box girder cross-sections.

These classical theories necessitate the representation of the applied loading by a Fourier Series, with the result that the computational effort required is still considerable, although very much less than that required in a full Finite Element solution. The Folded Plate Method is, however, very much more restricted in its range of application than the Finite Element Method and can only be applied to box girders in which the geometry of the cross-section remains constant all along the length. Also, in its basic form, the method can only deal with simply supported girders, but it has been extended by Scordelis to deal with girders spanning over intermediate supports, provided that the extreme ends of such girders still remain simply supported. However, since this extension of the method is based on a superposition technique this significantly increases the solution time required.

The Ordinary Method of folded plate analysis is an approximate method in which a simplified structural behaviour is assumed in order to reduce the amount of computation required in obtaining a solution. The present authors have previously shown [7], that, provided no concentrated loads are applied perpendicular to the planes of any of the plates, the errors introduced by these simplifying assumptions become very small provided that the length/width ratio of each component plate in the structure exceeds 3. Now, for the majority of box girder bridges, the dimensions of the component plates will be in accordance with this requirement.

SCORDELIS [6], has already proposed a method, known as the "Finite Segment Method", based on the assumptions of the Ordinary Method. In the Finite Segment Method, a process basically similar to that of the Finite Element Method is followed, each plate being divided initially into a number of rectangular elements which are subsequently assembled together. However, the simplifying assumptions of the Ordinary Method lead to much simpler element stiffness matrices and to many fewer nodal degrees of freedom and consequently to a much more economical solution process than the Finite Element Method. The solution time required by SCORDELIS' Finite Segment Method is of the same order as that required by his Folded Plate Method, but has the advantage of being able to deal with any support conditions. However, in the formulation as presented by SCORDELIS, the Finite Segment Method is restricted to the analysis of box girders in which the geometry

of the girder cross-section remains constant all along its span, the girders being loaded by longitudinal line loads only. Furthermore, no provision is made in the method for dealing with concentrated loads applied normal to the planes of the plates.

The Nodal Section Method is similar to the Finite Segment Method in that it is based on the Ordinary Method of folded plate analysis but its formulation is completely different and leads to further substantial savings of computer storage and time. The Nodal Section Method is not based on a conventional matrix stiffness approach but, instead, involves analysing the girder in a number of simple steps, similar to the steps that would be followed if the analysis was being carried out by hand. In fact, a hand analysis by the Nodal Section Method is a feasible proposition for many simple girders [8]. The advantages of the Nodal Section Method are that it can deal with various support conditions, makes use of a Finite Element plate bending solution to enable concentrated loads normal to the planes of the plates to be considered and, by employing an adaptation of a procedure suggested by JOHNSON and LEE [9] for folded plates, can be applied to the analysis of girders in which the geometry of the cross-section varies along the span. It thus combines a simple solution procedure with a wide field of application.

In the present paper, the basic theory of the Nodal Section Method is presented and results calculated by the method compared to theoretical solutions obtained using the Finite Element Method and other existing methods of analysis.

2. Basic Theory

The Nodal Section theory is based on the Ordinary Folded Plate Theory in which the only assumptions additional to those employed in a conventional elastic analysis are the following:

1. The bending action of an individual plate normal to its plane may be represented by considering a transverse one-way slab strip.
2. The in-plane longitudinal bending action of an individual plate is similar to that of a beam spanning between the end diaphragms.

On the basis of these assumptions, the behaviour of a box girder may be considered to consist of the action of a series of transverse one-way frames elastically supported by a system of interconnected plate beams spanning longitudinally between the supporting diaphragms. These frames only transmit shears and moments in the transverse direction, this action being termed the "transverse frame action", while the plate "beams" only transmit forces in their planes, this action being termed the "longitudinal plate action" of the structure. This idealised behaviour is illustrated in Fig. 2.

2.1. General Outline of Method

The transverse frame action is analysed by assuming each transverse frame to be supported at its joints, as shown in Fig. 2. By applying the slope-deflection equations it is possible to obtain the transverse moments acting within the frame, together with the joint reactions $R_B \ldots R_F$. The longitudinal plate action is then

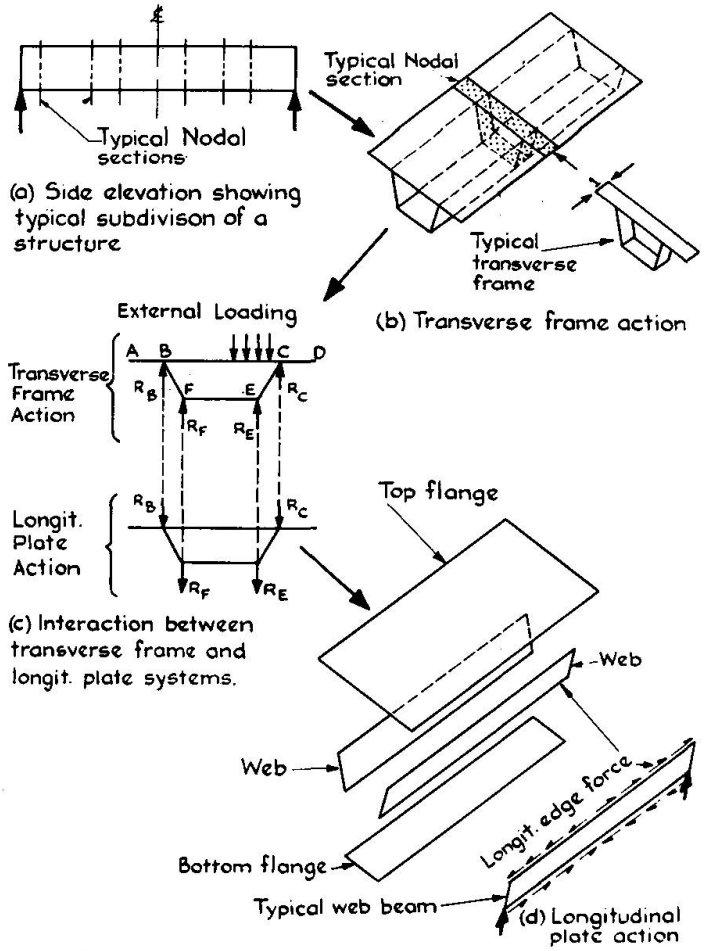

Fig. 2. Idealization of structural behaviour.

analysed by considering each plate to act as a beam spanning between the supporting diaphragms, the analysis ensuring that the longitudinal strain developed at the edge of each plate is compatible with the edge strain developed in adjacent plates and that the corresponding longitudinal edge forces in adjacent plates are in equilibrium as shown in Fig. 2. Furthermore, since the frame and plate systems are considered to be interconnected at the joints, as shown in Fig. 2, then the reactions of the frame system and the joint loads of the plate system must be equal and opposite, and the joint deflections of the two systems must be identical.

Since the Nodal Section Method is to be applied to box girders in which the geometry of the cross-section varies along the span, a transverse frame analysis is carried out at a number of sections taken on the structure, as shown in Fig. 2 the transverse frames being assigned a unit width in the longitudinal direction for convenience. The transverse sections are termed "nodal sections" and for a tapered girder, the frame taken at each nodal section will be of different dimensions and each frame is analysed under the action of the external loading pertaining to that particular nodal section. The reactions thus determined at each nodal section are then applied in the negative direction as joint loads on to the plate system and the longitudinal edge shear forces and strains set up in the plates at each nodal section are calculated and made to satisfy equilibrium and compatibility.

From the Nodal Section analysis, values of transverse bending moments, longitudinal stresses and vertical and horizontal joint displacements are determined at each nodal section. The basic method gives the values of these quantities at the joints only, but values at positions across the width of the various plates can also be determined by carrying out some additional simple steps.

Because equilibrium and compatibility conditions at the joints are only satisfied explicitly at the centre line of each of the nodal sections, the accuracy of the solution will vary with the number of nodal sections employed. It will be shown in Section 5 that the rate of convergence to an exact solution is rapid and that accurate results can be obtained with only a few nodal sections.

2.2. Special Consideration for Concentrated Loads

Further consideration must be given to the analysis of the transverse frame system under the action of the external loading. A one-way slab strip is only a good representation of the actual behaviour of a plate when the plate bends into an approximately cylindrical surface so that the proportion of the external load carried by longitudinal bending and twisting is negligible. This is so when the plate has a length/width ratio greater than 3, provided that the lateral loading has a reasonably uniform distribution in the longitudinal direction [7].

To deal with localised loading effects such as a wheel load on a top flange, the out-of-plane bending of each plate subjected to concentrated loading must first be analysed by the Finite Element Method. In this Finite Element analysis, the longitudinal edges of the plate are assumed to be fully clamped and the edge holding forces and moments are calculated. These fictitious holding forces are then applied in the negative direction to the box girder as joint "loads" and the box girder analysed by the Nodal Section Method.

Once the Nodal Section analysis has been completed, the results are then superimposed on to the initial Finite Element solution so that the fictitious edge holding forces and moments are eliminated.

In bridge design, it is often necessary to calculate the bending moments set up in the top flange in the locality of the applied concentrated loading. The initial Finite Element solution gives these moments, on the assumption that the longitudinal edges of the flange plate are clamped. To obtain the true values of these moments, another Finite Element plate bending solution of the loaded plate must be carried out after the Nodal Section analysis has been completed. In this final step, the deflections of the longitudinal edges of the plate, as predicted by the Nodal Section Method, are imposed on the plate, which is otherwise unloaded. By superimposing the results of the two Finite Element analyses, a complete picture of the moments set up in the loaded flange is obtained. The steps in a complete solution of this type are illustrated in Fig. 3.

The introduction of the Finite Element solution of the deck plates does, of course, increase the overall solution time. However, it must be appreciated that in the proposed procedure, a Finite Element solution is only required for those plates that are subjected to localised loading, and the number of plates loaded in this way is usually small compared to the total number of plates in the cross-section.

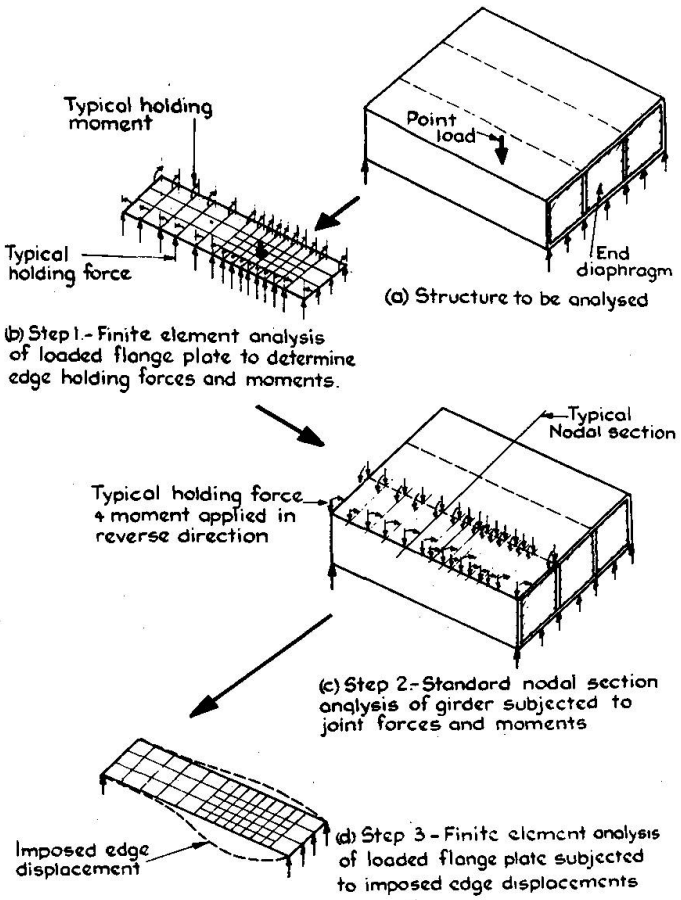

Fig. 3. Solution procedure for box girder subjected to point loading.

Furthermore, these plates are only analysed for bending normal to their planes so that only 3 degrees of freedom have to be considered at each nodal point instead of the 6 degrees of freedom that would have to be considered at each node in a full Finite Element analysis of the complete girder.

As an alternative to using the Finite Element Method, the edge holding forces of the plates subjected to concentrated loads may also be obtained from design tables [10]. The fictitious joint loads to be considered in the Nodal Section analysis may thus be determined directly without any additional solution time being required.

2.3 Sway Correction

Since, as discussed earlier, it is assumed that the frame system is *elastically* supported at the joints by the plate system, a situation is created in which the displacements of the plate system are produced by the frame reactions, whilst these reactions themselves depend partly on the plate displacements.

To overcome this problem, the Nodal Section analysis is divided into two parts. In the first part, which will be called the "No-Sway Solution", the box girder is analysed assuming the joints of the frame system to be *rigidly* supported by the plate system, whilst, at the same time, allowing the joints of the plate system to deflect.

The resulting incompatibilities between the deflections of the slab and plate systems are then removed by a subsequent "Sway Correction".

2.4. Continuous Box Girders

During the longitudinal plate analysis, each plate is analysed as a beam of variable cross-section spanning between the supporting diaphragms. If these beams are statically indeterminate, as in the case of a continuous girder, then a matrix approach is employed.

3. No-Sway Analysis

In this Section, the matrix formulation of the No-Sway analysis will be described. The analysis will be presented in general terms, but in some cases the equations will be written for the specific case of the typical structure shown in Fig. 4 to clarify their form. Only an outline of the various stages in the analysis can be given in the present paper, but greater detail of some of the steps has been included in earlier reports by the authors [11].

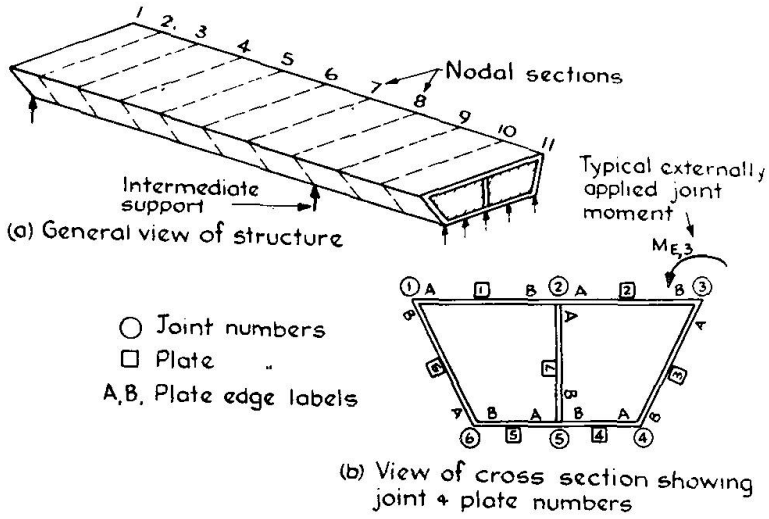

Fig. 4. Typical structure considered in the analysis.

3.1. Idealisation of Structure

Before the analysis can be started, the structural idealisation has to be carried out. First a number of nodal sections must be taken across the structure. These need not be equally spaced and should be distributed efficiently, i.e. more should be positioned in regions of anticipated high stress gradients as in a graded Finite Element mesh. In the general case, the nodal sections are numbered sequentially from 1 to n_o, a typical nodal section being denoted by n.

The next step is to define the cross-section of the structure. The plates are numbered from 1 to p_o, a typical plate being denoted by p and the joints are numbered from 1 to j_o, a typical joint being denoted by j. In addition, each longitudinal edge of each plate must be identified by the letter A or B, to assist the assembly procedure employed in the solution.

The following rules must be observed in carrying out the structural idealisation:

1. As will be discussed in Section 3.3, the method is only capable of dealing with structures in which no more than 3 plates meet at any joint, and 2 of these 3 plates must be co-planar. Consequently, a structure containing a joint such as that shown in Fig. 5 cannot be analysed, unless the joint is idealised as shown.

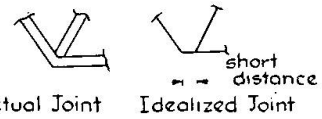

Fig. 5. Idealization of a typical 3 plate joint.

2. When a joint connects two plates only, then edge A of one plate and edge B of the other plate must be located at the joint, as at joints 1, 3, 4 and 6 of the structure illustrated in Fig. 4.
3. When a joint connects three plates, then edge A of one of the co-planar plates and edge B of the other co-planar plate must intersect at the joint. Either edge A or edge B of the third plate can be located at the joint, see joints 2 and 5 in Fig. 4.
4. In a structure containing adjacent co-planar plates, these plates must be numbered sequentially, see plates 1 and 2, and 4 and 5 in Fig. 4.

Having numbered and labelled the cross-section, a "connectivity" matrix $[AD]$ is set up, which specifies which edges of which plates meet at each joint. Each column of the matrix corresponds to a plate edge and each row corresponds to a joint, the plate edges meeting at a particular joint being indicated by inserting the figure "1" in the appropriate place in the matrix. The construction of the $[AD]$ matrix for the cross-section shown in Fig. 4 is as follows:

	Plate 1		Plate 2		Plate 3		Plate 4		Plate 5		Plate 6		Plate 7		
Edge	*A*	*B*	*A*	*B*	*A*	*B*	*A*	*B*	*A*	*B*	*A*	*B*	*A*	*B*	
$[AD]=$	1	0	0	0	0	0	0	0	0	0	0	1	0	0	Joint 1
	0	1	1	0	0	0	0	0	0	0	0	0	1	0	» 2
	0	0	0	1	1	0	0	0	0	0	0	0	0	0	» 3
	0	0	0	0	0	1	1	0	0	0	0	0	0	0	» 4
	0	0	0	0	0	0	0	1	1	0	0	0	0	1	» 5
	0	0	0	0	0	0	0	0	0	1	1	0	0	0	» 6

3.2 Transverse Frame Analysis

As discussed in Section 2.1, a transverse frame, such as that shown in Fig. 2, is analysed for transverse bending at each nodal section during the transverse frame analysis. This analysis is the same for each nodal section unless the nodal

section coincides with a diaphragm, which, by preserving the cross-sectional shape, prevents transverse bending occurring. Thus, for the typical structure shown in Fig. 4, nodal sections 1, 8 and 11 are supported by diaphragms, and a transverse frame analysis is not required at these sections.

The transverse frame analysis at a typical nodal section n will now be considered. It should be remembered that, in the No-Sway Solution now being discussed, those joints of the frame system which are *not* located at free edges are assumed to be rigidly supported by the plate system, so that no vertical or horizontal movements of these joints can occur, only transverse joint rotations being permitted. Joints located at cantilever free edges are considered to be unsupported.

Consider a typical plate p at a typical nodal section n, as shown in Fig. 6. The transverse span of the plate at this section is termed $s_{p,n}$, the thickness is termed $t_{p,n}$, the inclination to the horizontal $\varnothing_{p,n}$ and the modulus of elasticity $E_{p,n}$. The notation and the positive directions for the moments and rotations at the edges of the plate are as illustrated in Fig. 6, anticlockwise moments and rotations being considered positive.

In order to reduce the number of subscripts, the subscript n will be deleted whenever possible, because all expressions relate to the general nodal section n.

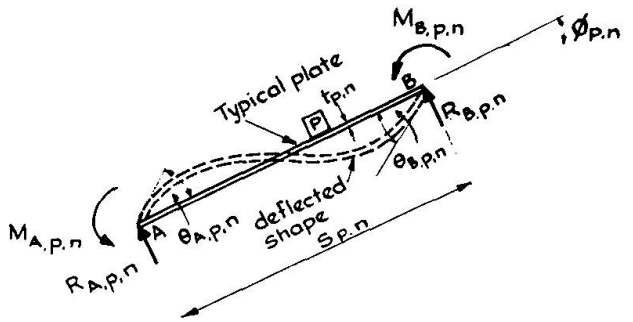

Fig. 6. Section through a typical plate p at nodal section n.

The *Slope Deflection Equations* for the typical plate p, see Fig. 6, may be written as:

$$\begin{aligned} M_{A,p} &= 2\lambda_p\,\theta_{A,p} + \lambda_p\,\theta_{B,p} + MF_{A,p} \\ M_{B,p} &= \lambda_p\,\theta_{A,p} + 2\lambda_p\,\theta_{B,p} + MF_{B,p} \end{aligned} \qquad (1)$$

$$\text{where } \lambda_p = \left(\frac{t^3 E}{6}\right)_p$$

An equation similar to (1) may be written for each plate in the cross-section from 1 to p_o, provided that the plate does not have a free edge. In the case of a plate, such as an edge cantilever, which does have a free edge, then, in equation (1), $\theta_{A,p} = \theta_{B,p} = 0$.

When equations similar to (1) have been written for *all plates* from $p = 1$ to p_o at the given nodal section they may be summarised as:

$$\{M\} = [A\theta]\,\{\theta\} + \{MF\} \qquad (2)$$

In this equation the vector $\{M\}$ represents all the plate edge moments, $\{\theta\}$ represents the vector for the plate edge rotations and $\{MF\}$ represents the vector

for the fixed end moments, thus for the typical structure shown in Fig. 4, each of these vectors contains 14 terms.

Clearly, the plate edge moments at any joint must be in equilibrium with any moment applied externally to that joint. For the particular case of the structure shown in Fig. 4, the equilibrium equation for joint 3 for example is:

$$M_{B,2} + M_{A,3} = M_{E,3}$$

Similar equilibrium equations may be written for each joint in the cross-section and the equations for the complete cross-section may be written in a general matrix form as:

$$\{\Sigma M\} = \{M_E\} \tag{3}$$

It will be seen that the required addition of the plate edge moments may be accomplished directly by using the $[AD]$ matrix defined in Section 3.1, as follows:

$$\{\Sigma M\} = [AD]\ \{M\} \tag{4}$$

Then, from equations (2), (3) and (4)

$$[AD]\ [A\theta]\ \{\theta\} + [AD]\ \{MF\} = \{M_E\} \tag{5}$$

Having satisfied equilibrium, the compatibility of the rotations at the joints must next be considered. This compatibility condition simply requires that the edge rotations of each plate meeting at a joint are identical.

For example, for the particular case of the structure shown in Fig. 4, using β_j to denote the joint rotation, the compatibility equation for joint 3 is:

$$\theta_{B,2} = \theta_{A,3} = \beta_3$$

It will be seen that the compatibility equations for the complete cross-section may again be established by using the $[AD]$ matrix as follows:

$$\{\theta\} = [AD]^T\ \{\beta\} \tag{6}$$

Substituting in equation (5)

$$[AD][A\theta][AD]^T\{\beta\} + [AD]\{MF\} = \{M_E\}$$

Defining, for convenience, a new matrix $[A\beta] = [AD][A\theta][AD]^T$, then:

$$[A\beta]\ \{\beta\} + [AD]\ \{MF\} = \{M_E\}$$

The only unknown in this equation is the vector $\{\beta\}$ representing the joint rotations and this may now be determined as:

$$\{\beta\} = -[A\beta]^{-1}\ ([AD]\ \{MF\} - \{M_E\}) \tag{7}$$

Knowing the joint rotations $\{\beta\}$, the plate edge rotations $\{\theta\}$ may then be determined from equation (6) and a further substitution back into the matrix form of the slope deflection equations, i.e. equation (2), yields the required values of the *Transverse Moments* $\{M\}$ acting at the plate edges at the typical nodal section *n*. From a consideration of these edge moments and the external load acting perpendicular to the plane of each plate, the transverse moments and the lateral displacements at positions across the width of each plate can be determined.

Once the transverse moments at the plate edges are known, the edge support reactions normal to the plane of each plate may be found. These are shown as $R_{A,p}$ and $R_{B,p}$ in Fig. 6 and for the typical plate they are given by:

$$\begin{aligned} R_{A,p} &= \frac{(M_A + M_B)}{s}_p + RF_{A,p} \\ R_{B,p} &= \frac{-(M_A + M_B)}{s}_p + RF_{B,p} \end{aligned} \tag{8}$$

Where the terms $RF_{A,p}$ and $RF_{B,p}$ represent the reactions due to the external loading acting on the span.

An equation similar to (8) may be written for all plates in the cross-section, other than edge cantilever plates, from 1 to p_o. These equations may be summarised as:

$$\{R\} = [AH]\ \{M\} + \{RF\} \tag{9}$$

so that the vector representing the edge reactions normal to the plane of each plate $\{R\}$ at the typical nodal section n may be determined. The vertical and horizontal components of these normal reactions may then be obtained by simple resolutions, and a vector $\{R_z^e\}$ containing the vertical components of the plate edge reactions and another vector $\{R_y^e\}$ containing the horizontal components of these reactions may be established. By using the $[AD]$ matrix once again, the total vertical and horizontal reactions at each joint may be obtained as:

$$\begin{aligned} &\text{vertical joint reactions} \quad \{RZ\} = [AD]\ \{R_z^e\} \\ &\text{horizontal joint reactions} \quad \{RY\} = [AD]\ \{R_y^e\} \end{aligned} \tag{10}$$

The transverse frame analysis is now complete for the typical nodal section n. The analysis is repeated for every nodal section, giving the transverse bending moments $\{M_n\}$ at each of these sections, together with the intensities of the vertical and horizontal reactions at the joints $\{Rz_n\}$ and $\{Ry_n\}$.

3.3. Linking Analysis

In this stage of the analysis, the joint reactions obtained from the transverse slab analysis are reversed in direction and then applied as joint loads on to the plate system. Since it is assumed that the plate system can only transmit forces in the planes of the various plates, the joint loads are resolved into their components in the planes of the plates to give the plate loads.

In the case of a joint at which more than 2 plates meet, the transverse frame reactions cannot be resolved into components in the direction of the intersecting plates, since only two equilibrium equations are available, i.e. the vertical and horizontal resolution of forces at the joint. However, if two of the three plates meeting at the joint are co-planar, then the total in-plane force component acting on these two plates can be determined and the analysis can be continued. The type of joint idealisation required to enable this restriction to be met has already been shown in Fig. 5.

3.4. *Longitudinal Plate Analysis*

In the longitudinal plate analysis, the plates are analysed as beams spanning between the supports and since the linking analysis is only able to provide the total plate load acting on any series of adjacent co-planar plates, such a system of co-planar plates is considered as one wide beam unit during the plate analysis. For the typical structure of Fig. 4, the beam units considered are as shown in Fig. 7, plates 1 and 2 being considered to act as a single beam, plates 4 and 5 being considered to act together as another single beam, and plates 3, 6 and 7 each being considered as an individual beam.

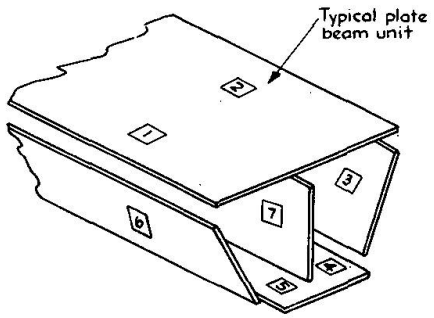

Fig. 7. Beam units considered during analysis of typical structure.

Thus, in the general case, a single plate beam unit considered during the longitudinal plate analysis may consist of several plates and may be connected to other units at its edges and also along several other lines within its width. A typical beam unit is shown in Fig. 8 this unit containing plates 1, 2...r...v. It is assumed that all the co-planar plates within the beam unit are numbered consecutively (in accordance with restriction 4 in Section 3.1), and that at the typical nodal section n, each co-planar plate has the same thickness ($t_{1,n} = t_{2,n} \ldots = t_{r,n} \ldots = t_{v,n}$) and the same elastic modulus ($E_{1,n} = E_{2,n} \ldots = E_{r,n} \ldots = E_{v,n}$). However, the theory can be adapted to accommodate different thicknesses, etc.

During the longitudinal bending, the forces shown in Fig. 8 will be set up at the typical nodal section n of the beam unit, this nodal section being assumed to

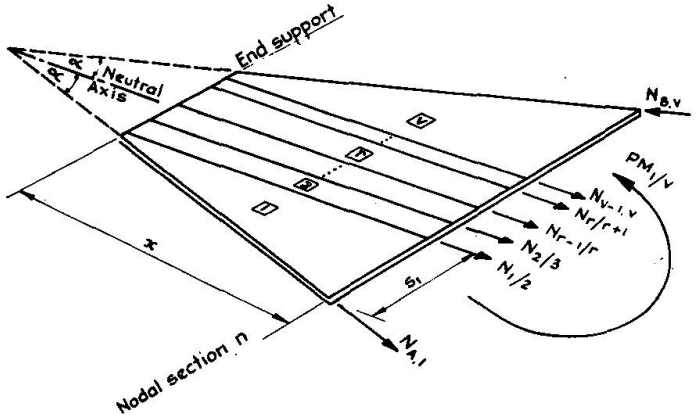

Fig. 8. Forces set up in a typical plate beam unit containing several co-planar plates.

be at a distance x from the end of the beam. For clarity, the suffix n relating to the nodal section will be omitted from the following equations, but it should be remembered that these equations relate to nodal section n. The forces set up are:

1. Longitudinal forces $N_{A1}, N_{1/2} \ldots N_{r/r+1} \ldots N_{Bv}$ set up along the lines at which the beam unit is connected to adjacent web units. These forces are set up by virtue of the longitudinal shear developed between the adjacent units, this shear being assumed to have an intensity U_{A1}, $U_{1/2} \ldots U_{r/r+1} \ldots U_{Bv}$ at the various joints. The positive directions of these forces are shown in Fig. 8, all the forces, apart from N_{Bv} being positive when tensile.
2. A bending moment $PM_{1/v}$ set up by the total in-plane plate load acting on the beam unit as obtained from a resolution of the transverse frame reactions. This moment is calculated assuming the beam unit to be completely disconnected from all other beam units, and is defined as positive when it is a sagging moment, as shown in Fig. 8.

Having defined the forces acting on the section, the longitudinal bending stresses set up by these forces at nodal section n can now be calculated from beam theory. In the first instance, the bending stresses parallel to the neutral axis of the beam unit will be calculated. It will be appreciated that with a tapered web beam the neutral axis of the beam will be inclined to the horizontal at an angle α as defined in Fig. 8. For convenience, define $H = s_1 + s_2 \ldots s_r \ldots + s_v$ and let $t = t_1 = t_2 \ldots = t_r \ldots = t_v$.

Total moment (sagging positive) on cross-section

$$M = PM_{1/v} + N_{A,1} \tfrac{H}{2} \cos\alpha + N_{1/2} \left(\tfrac{H}{2} - s_1\right) \ldots + N_{r/r+1} \left(\tfrac{H}{2} - (s_1 + s_2 \ldots + s_r)\right) \ldots + N_{B,v} \tfrac{H}{2} \cos\alpha \tag{11}$$

Total axial force (tension positive) on cross-section =

$$= N_{A,1} \cos\alpha + N_{1/2} \ldots + N_{r/r+1} \ldots - N_{B,v} \cos\alpha$$

Thus knowing the bending moment and axial forces acting on the section from equation (11) the total longitudinal stresses set up at all points across the section can now be determined from standard beam theory. For example, for the typical case of a single plate "p", which does not form part of a co-planar plate unit, the stress acting at edge "A" is as given in equation (12).

$$\bar{\sigma}_{A,p} = \frac{6}{t_p s_p^2} PM_p + \frac{4}{t_p s_p} N_{A,p} \cos\alpha_p + \frac{2}{t_p s_p} N_{B,p} \cos\alpha_p \tag{12}$$

The stresses at the edge of the typical plate, i.e. $\bar{\sigma}_{A,p}$ and $\bar{\sigma}_{B,p}$ calculated according to equation (12), act parallel to the neutral axis of the plate. Before equilibrium and compatibility between this and adjacent plates can be considered these stresses must be converted into stresses along the edges of the plate unit. The resolution at edge A of plate p is illustrated in Fig. 9 and the stress along this edge at section n may be written as:

$$\sigma_{A,p} = \frac{\bar{\sigma}_{A,p}}{\cos^2\alpha_p} - \frac{2U_{A,p} \tan\alpha_p}{t_p} \tag{13}$$

and a similar equation may be written for edge B of the plate.

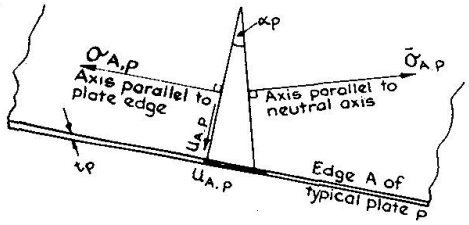

Fig. 9. Resolution of stresses at typical plate edge.

Thus, for the typical plate beam unit at nodal section n, by using equations (12) and (13) a relationship can be established between stresses (σ) and hence the strains (ε) set up along all the lines at which the unit is connected to adjacent beam units and the longitudinal shear forces (N) and the distributed shear forces (U) acting along these lines, together with the bending moment (PM) that would be set up in the unit assuming it to be completely disconnected from adjacent units.

Similar relationships may be established for all other plate beam units within the cross-section. If the beam unit has a free edge, as in the case of an edge cantilever, then the expressions must be modified to allow for the fact that no shear forces exist along this edge.

When the expressions have been established for all units at nodal section n, they may be written in a matrix form as follows:

$$\{\varepsilon\} = [SN]\ \{N^e\} + \{MO\} - [SU]\ \{U^e\} \tag{14}$$

For the typical cross-section shown in Fig. 4, the strain vector $\{\varepsilon\}$ for nodal section n will contain terms in the following order:

$$\varepsilon_{A,1};\ \varepsilon_{1/2};\ \varepsilon_{B,2};\ \varepsilon_{A,3};\ \varepsilon_{B,3};\ \varepsilon_{A,4};\ \varepsilon_{4/5};\ \varepsilon_{B,5};\ \varepsilon_{A,6};\ \varepsilon_{B,6};\ \varepsilon_{A,7} \text{ and } \varepsilon_{B,7}.$$

At a joint between between adjacent beam units, the strains along the joint must satisfy compatibility. For example, for the typical cross-sections shown in Fig. 4, the strain compatibility equation for Joint 3 at the typical nodal section n becomes:

$$\varepsilon_{B,2} + \varepsilon_{A,3} = 0$$

The compatibility equations for the complete cross-section at nodal section n may be written as:

$$\{\Sigma\varepsilon\} = 0 \tag{15}$$

It will be seen that the required addition of the plate edge strains can be carried out by setting up a matrix, that will be denoted by $[AD^1]$, which is a modified form of the $[AD]$ matrix defined earlier. For the typical structure shown in Fig. 4, $[AD^1]$ has the following form:

$$[AD^1] = \begin{bmatrix} 1 & 0 & 0 & 0 & 0 & 0 & 0 & 0 & 0 & 1 & 0 & 0 \\ 0 & 1 & 0 & 0 & 0 & 0 & 0 & 0 & 0 & 0 & -1 & 0 \\ 0 & 0 & 1 & 1 & 0 & 0 & 0 & 0 & 0 & 0 & 0 & 0 \\ 0 & 0 & 0 & 0 & 1 & 1 & 0 & 0 & 0 & 0 & 0 & 0 \\ 0 & 0 & 0 & 0 & 0 & 0 & 1 & 0 & 0 & 0 & 0 & 1 \\ 0 & 0 & 0 & 0 & 0 & 0 & 0 & 1 & 1 & 0 & 0 & 0 \end{bmatrix}$$

and the required addition may be obtained as:

$$\{\Sigma\varepsilon\} = [AD^1]\ \{\varepsilon\} = 0 \tag{16}$$

Then, substituting for $\{\varepsilon\}$ from equation (14):

$$[AD^1]\ [SN]\ \{N^e\} + [AD^1]\ \{MO\} - [AD^1]\ [SU]\ \{U^e\} = 0 \tag{17}$$

Also, at a joint between two plate beam units, in addition to the strain compatibility condition the shear forces along the joint must satisfy equilibrium.

For the typical cross-section shown in Fig. 4, the shear force equilibrium for joint 3 for example is as follows:

$$N_{B,2} = N_{A,3} = N_3$$

It will be seen that the shear equilibrium equations for the complete cross-section may again be established by using the $[AD^1]$ matrix as follows:

$$\{N^e\} = [AD^1]^T\ \{N\} \tag{18}$$

Similar equilibrium equations may be written for the distributed shear forces acting along the edge, i.e.

$$\{U^e\} = [AD^1]^T\ \{U\} \tag{19}$$

Substituting from equations (18) and (19) in equation (17) yields:

$$[AD^1][SN][AD^1]^T\ \{N\} + [AD^1]\ \{MO\} - [AD^1][SU][AD^1]^T\ \{U\} = 0 \tag{20}$$

Defining, for convenience, two new matrices and a new vector:

$$[DN_n] = [AD^1]\ [SN]\ [AD^1]^T$$
$$[DU_n] = [AD^1]\ [SU] \text{ and } [DO_n] = [AD^1]\ \{MO\}$$

Then, reintroducing the suffix n to show that the terms relate to the typical nodal section n, equation 20 may be re-written as:

$$[DN_n]\ \{N_n\} + \{DO_n\} - [DU_n]\ \{U_n\} = 0 \tag{21}$$

There are two unknowns in this equation, viz. the vectors $\{N_n\}$ and $\{U_n\}$ which represent, respectively, the total longitudinal shear force and the intensity of the longitudinal shear force at each joint at the nodal section n. Another relationship between these two vectors must be established before the equations can be solved.

Such a relationship will now be obtained by considering nodal section n on a typical joint j. Let a co-ordinate axis z be taken along this joint, as shown in Fig. 10a, the distance along the joint between adjacent nodal sections then being $l_{z,n-1}$, $l_{z,n}$, etc. By considering an elemental length δz of the joint, as in Fig. 10b at at a distance z from the end support, it is apparent that, $U(z) = dN(z)/dz$.

A portion of a typical curve representing the longitudinal distribution of the joint shear forces is shown in Fig. 10a. Assume that the curve may be represented by a polynomial function:

$$N(z) = N_n + a_1\ z + a_2\ z^2$$

the origin of the z co-ordinate axis being assumed to be located at section n.

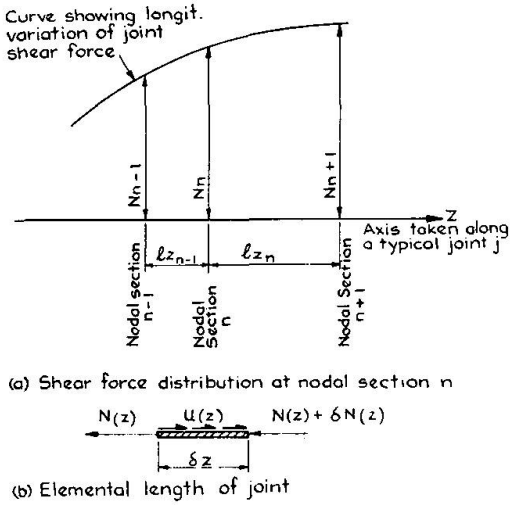

Fig. 10. Distribution of shear forces along typical joint.

$$\text{Then } U(z) = a_1 + 2\ a_2\ z \tag{22}$$

and by determining the values of the coefficients $a_1 + a_2$ from the values of N at each section, the value of U_n may be determined from equation (22) as:

$$U_n = N_{n-1}\frac{-l_{zn}}{l_{zn-1}\,(l_{zn-1}+l_{zn})} + N_n\frac{(l_{zn}-l_{zn-1})}{l_{zn}\,l_{zn-1}} + N_{n+1}\frac{l_{zn-1}}{l_{zn}\,(l_{zn-1}+l_{zn})} \tag{23}$$

A similar equation may be written for each other joint at nodal section n and these equations may be summarised as:

$$\{U_n\} = [LB_n]\ \{N_{n-1}\} + [LC_n]\{N_n\} + [LF_n]\{N_{n+1}\} \tag{24}$$

Equation (24) gives the required additional relationship between the $\{U_n\}$ and $\{N_n\}$ vectors,
Substituting for $\{U_n\}$ in equation (21) gives:

$$[DN_n]\ \{N_n\} + \{DO_n\} - [DU_n]\ [LB_n]\ \{N_{n-1}\} - [DU_n]\ [LC_n]\ [N_n] - [DU_n]\ [LF_n]\ \{N_{n+1}\} = 0$$

This equation may be written as:

$$[DB_n]\ \{N_{n-1}\} + [DC_n]\ \{N_n\} + [DF_n]\ \{N_{n+1}\} = -\{DO_n\} \tag{25}$$

Where

$$[DC_n] = [DN_n] - [DU_n]\ [LC_n];$$
$$[DB_n] = -[DU_n]\ [LB_n] \text{ and } DF_n = -[DU_n]\ [LF_n]$$

Equation (25) relates to the typical nodal section n only and similar equations may be established for each nodal section and all the equations thus obtained arranged in matrix form. Equation (26) illustrates the form of these equations for 3 typical nodal sections: $n-1$, n and $n+1$.

$$\begin{bmatrix} [DB_{n-1}] & [DC_{n-1}] & [DF_{n-1}] & & \\ & [DB_n] & [DC_n] & [DF_n] & \\ & & [DB_{n+1}] & [DC_{n+1}] & [DF_{n+1}] \end{bmatrix} \begin{Bmatrix} \{N_{n-1}\} \\ \{N_n\} \\ \{N_{n+1}\} \end{Bmatrix} = - \begin{Bmatrix} \{DO_{n-1}\} \\ \{DO_n\} \\ \{DO_{n+1}\} \end{Bmatrix} \quad (26)$$

The equations for the complete structure, i.e. for all nodal sections, can be summarised as shown in equation (27) and by inverting the $[AA]$ matrix, the joint shear forces can be obtained as shown in equation (28).

$$[AA]\ \{N\} = \{M\} \quad (27)$$

$$\{N\} = [AA]^{-1}\ \{M\} \quad (28)$$

The terms of the vector $\{N\}$ represent the shear forces at each joint at each nodal section. The joint shear forces relating to any one nodal section, e.g. $\{N_n\}$, can then be extracted from the $\{N\}$ vector and the shear forces at the edges of the individual plates, i.e. $\{N^e\}$, determined, as in equation (18).

Knowing the longitudinal edge shear forces acting on each individual plate, the *Longitudinal Stresses* at the edges of each plate acting parallel to the neutral axis of the plate can then be determined from equation (12). Since in equation (12) these stresses are assumed to be linearly distributed across the width of each plate the stress at any point across the width of the plate can be determined once the edge stresses are known.

Since the stress distribution and therefore the bending moment acting at all sections of each of the plate beam units is now known, the deflection of each individual plate can be determined using normal beam theory. Once all the in-plane plate deflections are known, the *Vertical* and *Horizontal Displacements* of the joints may be obtained from a simple resolution procedure.

The Nodal Section No-Sway Analysis is now complete. During the analysis the following quantities have been calculated at each nodal section:

1. The transverse bending moments at the plate edges and at any required position across the width of each plate.
2. The longitudinal stresses at the plate edges and at any required position across the width of each plate.
3. The deflection normal to the plane and the deflection in the plane of each plate at any required position across the width of the plate.
4. The vertical and horizontal displacement of each joint.

These quantities present a comprehensive picture of the behaviour of the box girder.

4.0. Sway Correction

During the No-Sway analysis described in Section 3, the transverse frame action was analysed assuming the one-way slab strips to be rigidly supported at the longitudinal joints of the girder, whereas, in the longitudinal plate analysis, these joints were allowed to deflect and their deflections were calculated. Consequently, incompatibilities exist between the joint displacements of the plate and frame systems and the object of the Sway Correction is to remove these incompatibilities.

There are two methods by which the Sway Correction may be accomplished. The first of these methods is based on the "Method of Particular Loadings"

developed by YITZHAKI [4] for folded plate structures and this provides a closed-form solution, which is applicable to all girders, but which considerably increases demands on computer time and storage space. The second method employs an iterative technique and does not lead to any increased demands on computer storage space and converges in all cases, the rate of convergence depending on the form of the girder cross-section.

The authors have investigated the use of both methods and have found that the iterative technique is the most suitable for a method of analysis that is to be used in a design office. An adaptation of the Standard Iterative Technique used in folded plate structures was first tried but was found to be unsatisfactory since, in some instances, the rate of convergence was very slow and, in some particular cases, the solution was found to be divergent. As a result of this an improved "Accelerated Iterative Technique" based upon a method established by MAST [12] for folded plates has been developed and Fig. 11 shows how, for a typical girder, the accelerated iterative process rapidly converges to the correct solution where as the normal iterative procedure does not.

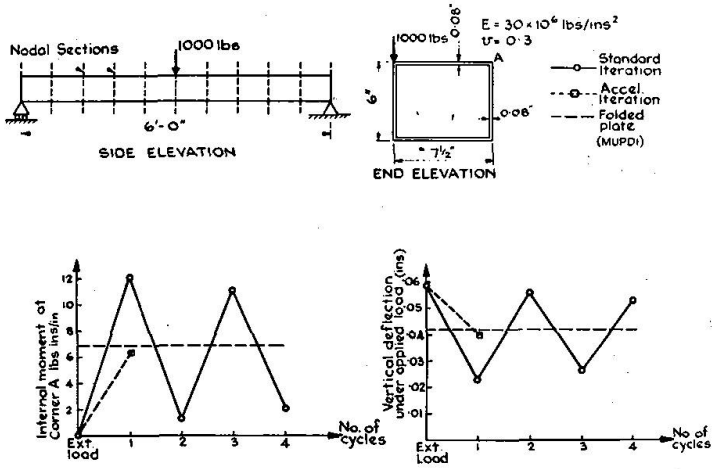

Fig. 11. Comparison of rates of convergence of standard iteration and accelerated iteration sway correction procedures.

The first step in the Sway Correction is to quantify the incompatibilities between plate and frame displacements, arising from the No-Sway Analysis. A convenient way of doing this is to express the incompatibilities in terms of the "relative joint displacements" or "sway displacements" of each component plate. The sway displacement for a typical plate p at nodal section n, i.e. $\Delta_{p,n}$ is defined in Fig. 12a.

Hence, the in-plane plate displacements $v_{p,n}$ and the vertical and horizontal joint displacements $\delta v_{j,n}$ and $\delta h_{j,n}$, obtained from the No-Sway Analysis, must now be converted, by means of simple geometry, into equivalent sway displacements $\Delta_{p,n}$ for the various plates and these sway displacements must be determined at each nodal section that does not coincide with the position of a supporting diaphragm. At a diaphragm position, all such sway displacements are prevented. Clearly should any plate have a free edge, such as an edge cantilever plate, then a sway displacement will not be set up within the plate.

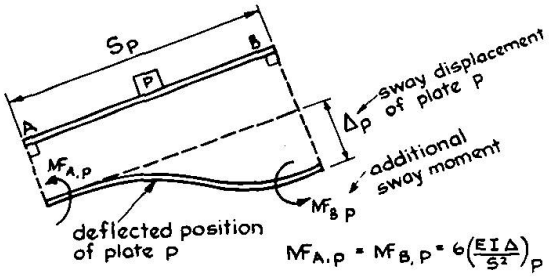

Fig. 12a. Definition of sway displacement of typical plate p at nodal section.

4.1. The Accelerated Iteration Method

It must be remembered that the object of the Sway Correction is to remove the incompatibilities existing between the displacement of the frame and plate systems at the end of the No-Sway Analysis for the external load condition. Defining the incompatibility for a typical plate as:

incompatibility=sway displacement of plate in plate system minus the sway displacement of plate in frame system (29)

then, since in the No-Sway analysis for the girder under external loading, the joints of the frame system are assumed to be non-deflecting, the incompatibility (β) for a typical plate p at nodal section n arising from the No-Sway analysis is:

$$\beta_{p,n}^{Ext} = \Delta_{p,n}^{Ext} - 0 \tag{30}$$

where the superscript *Ext* denotes that the incompatibilities relate to the No-Sway Analysis.

The *first cycle* of the Accelerated Iteration Method is now commenced. Sway deformations equal to the incompatibilities ($\Delta_{p,n}^{Ext}$) which exist at the end of the external load analysis are imposed on each member of the frame system at each nodal section. These imposed deformations set up additional transverse moments within the members and another No-Sway Analysis is now carried out as described in Section 3. From this analysis, additional sway displacements ($\Delta_{p,n}^{I}$) are calculated for the plate system. Then, according to equation (29), the incompatibilities arising from the first cycle may be defined as:

$$\beta_{p,n}^{I} = \Delta_{p,n}^{I} - \Delta_{p,n}^{Ext} \tag{31}$$

One of the unwanted incompatibilities corresponding to the external loading, as determined from equation (30), may now be removed by superimposing the incompatibilities obtained from the first cycle, as listed in equation (31), in the correct proportion. Any incompatibility may be chosen for removal; for example, to remove the incompatibility in plate 4 at nodal section 6, then:

$$\beta_{4,6}^{Ext} + \mu_I^I(\beta_{4,6}^{I}) = 0 \text{ therefore } \mu_I^I = -\frac{\beta_{4,6}^{Ext}}{\beta_{4,6}^{I}} \tag{32}$$

μ_I^I defining the proportion of the values from the first cycle that must be superimposed on to the external load values.

The complete solution at the end of the first cycle may now be obtained as:

$$\text{Complete solution} = \text{external load solution} + \mu_I^I \text{ (first cycle solution)} \tag{33}$$

Also, the incompatibilities remaining at the end of the first cycle may be determined as:

$$\beta_{p,n}^{I'} = \beta_{p,n}^{Ext} + \mu_I^I (\beta_{p,n}^I) \tag{34}$$

the remaining incompatibility for plate 4 at nodal section 6 now being zero.

In the *second cycle* of the Accelerated Iteration Method, sway deformations equal to the incompatibilities that exist at the end of the first cycle, as in equation (34), are imposed on the slab system. Another No-Sway Analysis is carried out and additional sway displacements ($\Delta_{p,n}^{II}$) are calculated. Then, from equation (29), the incompatibilities arising from the second cycle are:

$$\beta_{p,n}^{II} = \Delta_{p,n}^{II} - \beta_{p,n}^{I'} \tag{35}$$

A superposition of a certain proportion (μ_{II}^{II}) of these incompatibilities, together with a certain proportion (μ_I^{II}) of the first cycle incompatibilities, from equation (31), will enable any two of the unwanted incompatibilities corresponding to the external loading listed in equation (30), to be removed.

For example, if the incompatibilities of plates 4 and 9 at nodal section 6 are chosen for removal, then:

$$\begin{aligned} &\textit{for plate 4} \quad \beta_{4,6}^{Ext} + \mu_I^{II} (\beta_{4,6}^I) + \mu_{II}^{II} (\beta_{4,6}^{II}) = 0 \\ &\textit{for plate 9} \quad \beta_{9,6}^{Ext} + \mu_I^{II} (\beta_{9,6}^I) + \mu_{II}^{II} (\beta_{9,6}^{II}) = 0 \end{aligned} \tag{36}$$

From these equations, the values of the proportions μ_I^{II} and μ_{II}^{II} may be determined and then the complete solution at the end of the second cycle may be obtained as:

$$\begin{aligned} \text{Complete solution} = \text{external load solution} &+ \mu_I^{II} (\text{1st cycle solution}) \\ &+ \mu_{II}^{II} (\text{2nd cycle solution}) \end{aligned} \tag{37}$$

Also, the incompatibilities remaining at the end of the second cycle may be determined as:

$$\beta_{p,n}^{II'} = \beta_{p,n}^{Ext} + \mu_I^{II} (\beta_{p,n}^I) + \mu_{II}^{II} (\beta_{p,n}^{II}) \tag{38}$$

the remaining incompatibilities on both plates 4 and 9 at nodal section 6 now being zero.

A *third cycle* of the Accelerated Iteration Method may now be carried out, in which sway deformations equal to the incompatibilities that exist at the end of the second cycle are applied to the frame system and another No-Sway Analysis of the girder carried out. This third cycle will provide a further set of incompatibilities which, when taken in conjunction, with those obtained from the first and second cycles, will enable any three of the initial incompatibilities corresponding to the external loading to be removed. Thus, a solution of greater accuracy may be obtained after the third cycle.

Further iterative cycles may be carried out, each successive cycle commencing with the application to the frame system of sway deformations equal to the incompatibilities remaining at the end of the previous cycle. In each cycle, a

No-Sway Analysis of the girder has to be carried out, and each cycle provides a new set of incompatibilities which enables one more of the original incompatibilities, arising from the external load analysis, to be eliminated. In order to remove all these original incompatibilities and thus provide an exact solution, the total number of iterative cycles required is theoretically equal to the product of the number of plates in the cross-section and the number of nodal sections taken, i.e. $p_o \times n_o$, and the last of these cycles would involve the solution of $p_o \times n_o$ simultaneous equations.

However, in practice it is found that, by virtue of the nature of the deformations set up in the box girder, the elimination of one particular incompatibility leads to the simultaneous elimination of several others, so that an accurate solution can be obtained by taking very many fewer cycles than are theoretically necessary for an exact solution. The reasons for this are two-fold:

In the first place, any set of sway displacements set up will have a variation over the length of the girder which is a function of the elastic properties of the girder. Thus, any set of sway displacements such as Δ^I, set up by another set of sway displacements, such as Δ^{Ext} will have a longitudinal distribution similar to the original set and the ratio of Δ^I to Δ^{Ext} will be almost the same at each nodal section. Consequently, when the incompatibilities are eliminated from a particular plate at a particular nodal section, they are also made extremely small at all the other nodal sections on that plate. Thus, accurate results may be obtained by considering the removal of incompatibilities at a few nodal sections only; in many cases it has been found sufficient to remove the incompatibilities at only one nodal section and in no case has the removal of the incompatibilities at more than two nodal sections been found necessary in order to provide a convergent solution.

Secondly, within any closed cell of the cross-section, the relationship between the sway displacement of any one plate and the sway displacements of the other plates within the cell is dependent on the resistance of the girder cross-section to distortion. For any set of sway displacements, such as Δ^I, set up by another set of sway displacements, such as Δ^{Ext}, the ratio of Δ^I to Δ^{Ext} will be similar for each plate within the closed region. Consequently, when the incompatibilities are removed from any one plate within the closed cell, they are also greatly reduced for all the other plates within the cell.

Satisfactory convergence of the Accelerated Iteration Method can thus be achieved by removing the incompatibilities at one or two nodal sections only and carrying out one iterative cycle for each closed cell within the cross-section, together with one cycle for any other plates that may exist in the cross-section. Thus, for a multi-cell girder, where the cross-section effectively forms only one closed region, one iterative cycle only is required. For a girder containing discreet cells, such as that shown in Fig. 12b, one iterative cycle is required for each box, together with an additional cycle for each connecting flange, so that three iterative cycles are required in this particular case. The order in which the 3 cycles are carried out is immaterial as illustrated in the convergence plot shown in Fig. 12b.

When all the required iterative cycles have been completed for a given section, the final results for the complete girder are obtained by superimposing the appropriate proportion of the values calculated in each cycle on to the original values obtained from the external load analysis.

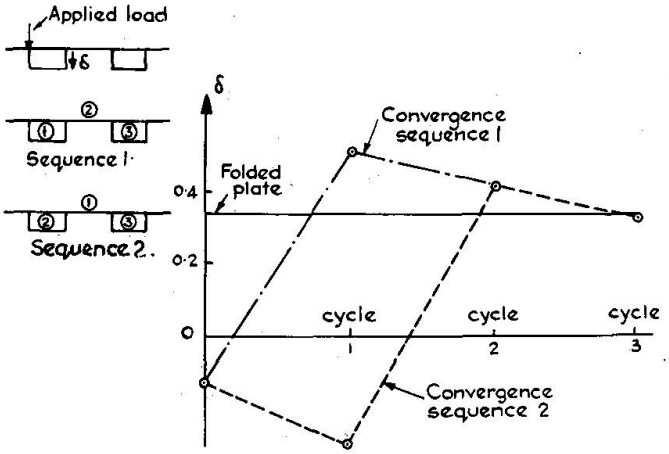

Fig. 12b. Illustration of convergence of solution for discreet cell girder.

5. Discussion of Results

In this section, the accuracy of the Nodal Section Method will be assessed by analysing several different types of girders subjected to different loading and support conditions and comparing the results obtained from the Nodal Section Method with those results obtained from a full three-dimensional Finite Element analysis and also to results obtained from the Folded Plate Method (MUPDI) developed by Scordelis. Both these methods are currently widely used in box girder analysis and their accuracy, within their particular fields of application, has been firmly established.

The first type of girder considered will be the simply-supported, single-cell girder shown in Fig. 13. A full parametric study of such girders has been carried out by the authors [14] in which 20 girders of differing dimensions were analysed, the girder dimensions and proportions being chosen on the basis of a statistical survey of the girders currently in service. All these girders were subjected to a line

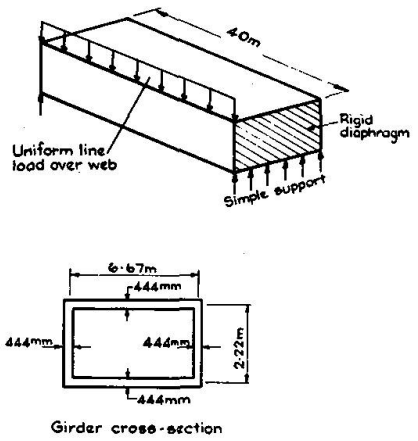

Fig. 13. Details of typical single-cell girder.

loading applied over one web, as shown in Fig. 13, since such a loading would tend to set up gross cross-sectional deformations and would thus provide a good test of the accuracy of the Nodal Section Method.

The extensive results obtained from this parametric study have been presented in detail in a separate report [14] and cannot be repeated here. However, a sample of the results will be presented for the girder having the dimensions shown in Fig. 13 and this girder may be regarded as a typical single-cell girder, since its proportions closely represent the most frequently occurring proportions observed during the statistical survey of practical girders.

Since both the Finite Element and Nodal Section methods require an idealisation of the structure, convergence tests were carried out first of all for the typical girder to determine the accuracy obtainable from various idealisations. The finite element meshes and nodal section positions considered are shown in Fig. 14 and the results of the convergence tests are summarised in Fig. 15 where the predicted transverse moments and longitudinal stresses at the loaded joint at the mid-span cross-section are compared to values given by the folded plate method. The results show clearly that both methods converge rapidly and that for the particular loading case considered, reasonably accurate results can be obtained by taking 5 nodal sections only.

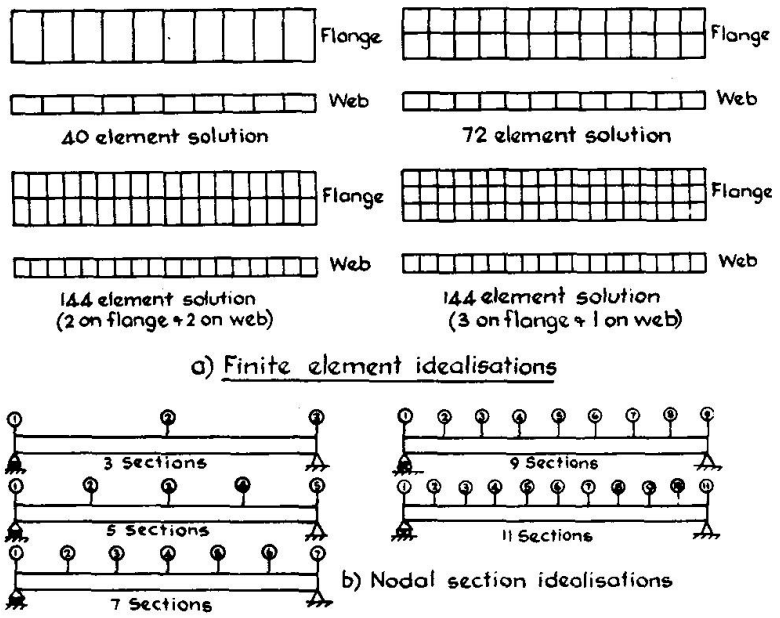

Fig. 14. Idealisations considered in convergence tests.

In each Nodal Section Analysis, two cycles of the sway correction procedure were carried out since it has been found that two cycles are necessary in order to obtain accurate values of the transverse moments for concrete girders in which the resistance to cross-sectional deformations is high. The longitudinal stresses and deflections of both concrete and steel girders and also the transverse moments of steel girders are obtained accurately after 1 sway correction. In no case during the parametric study of single-cell girders was it found necessary to employ more than 2 cycles of the sway correction procedure.

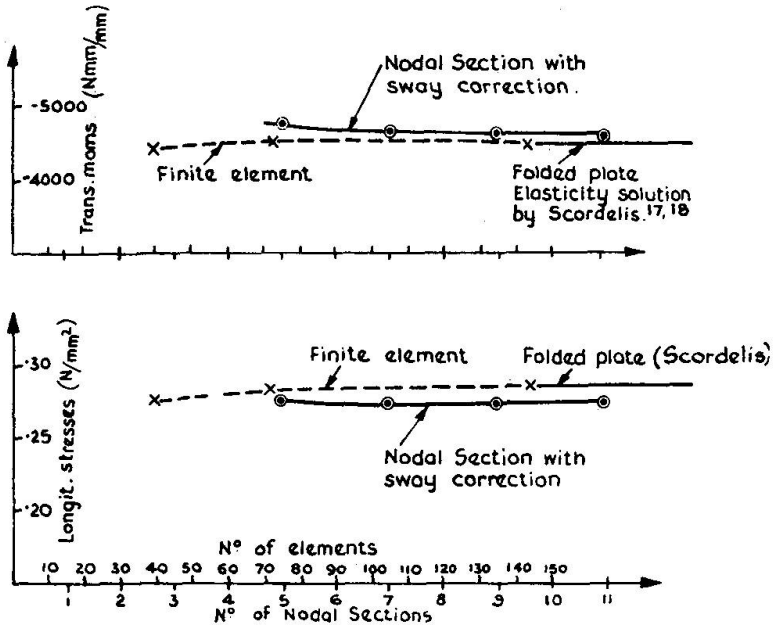

Fig. 15. Convergence of transverse moments and longitudinal stress values for a typical single-cell girder.

In Fig. 16 the Finite Element and Nodal Section solution times for the parametric study are plotted, and this diagram illustrates clearly the main disadvantage of the finite element method in a design context. For the finest mesh considered in the analysis, i.e. the mesh containing 144 elements, a solution time of 20 minutes was required on an I.C.L. System 470 computer, whereas the comparable time for the Nodal Section solution employing 11 sections and 2 sway corrections, was of the order of 1 minute. The finite element mesh containing 144 elements, whilst being more than adequate to provide accurate results for the simply supported single-cell girder of Fig. 13, would certainly not be sufficient for the analysis of multi-cell, multi-span girders and the use of larger meshes for such structures would make the Finite Element Solution time prohibitive in any design study.

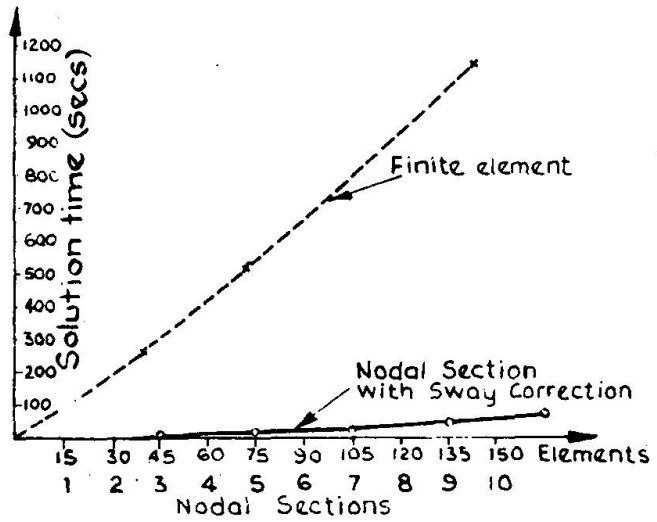

Fig. 16. Comparison of solution times for a typical single-cell girder.

In addition to the actual computer time used, the Finite Element Solution also requires a great deal of data preparation time. The 144 element mesh used in the present investigation required the preparation of some 300 computer cards, compared to the preparation of some 25 cards for the comparable Nodal Section Solution, and this is another serious disadvantage of the Finite Element Method in any design application.

Since the values given in Fig. 15 relate to the loaded corner of the girder only, the transverse moments, longitudinal stresses and vertical deflections for the complete central cross-section are shown in Fig. 17 and it is seen that the distributions predicted by the Nodal Section and Folded Plate methods agree closely.

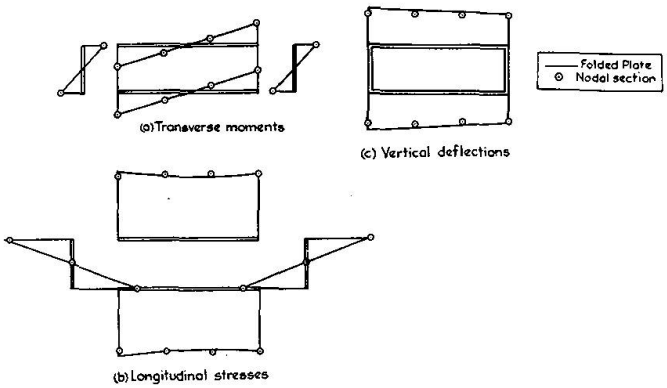

Fig. 17. Distribution around mid-span cross-section of typical girder.

Figures 15 and 17 shown the accuracy obtainable with the Nodal Section Method for one typical girder only. Obviously, as the girder proportions were varied during the parametric study, significant changes occurred in the structural behaviour, but, in all cases, the accuracy of the Nodal Section solution was maintained. An example of this is given in Fig. 18 where the effects of varying the

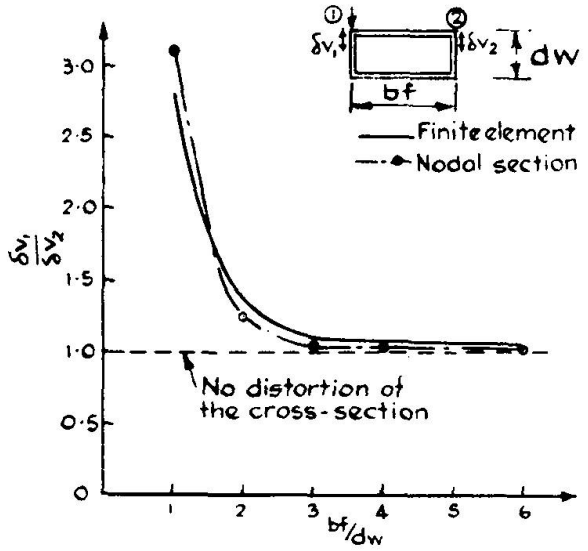

Fig. 18. Variation in ratio of vertical web deflections with variation in flange width/web depth ratio (bf/dw).

flange width/web depth parameter are illustrated. The amount of cross-sectional deformation under load is seen to vary rapidly with a change of this parameter, but the curves obtained from the nodal section and finite element solutions are seen to agree closely throughout the complete range considered.

In addition to single-cell girders, the two types of girder shown in Fig. 19 were also analysed. Since, as discussed earlier, the finite element solution times for such girders would be prohibitive, the Nodal Section values will in both cases be compared to results obtained from the Folded Plate Method.

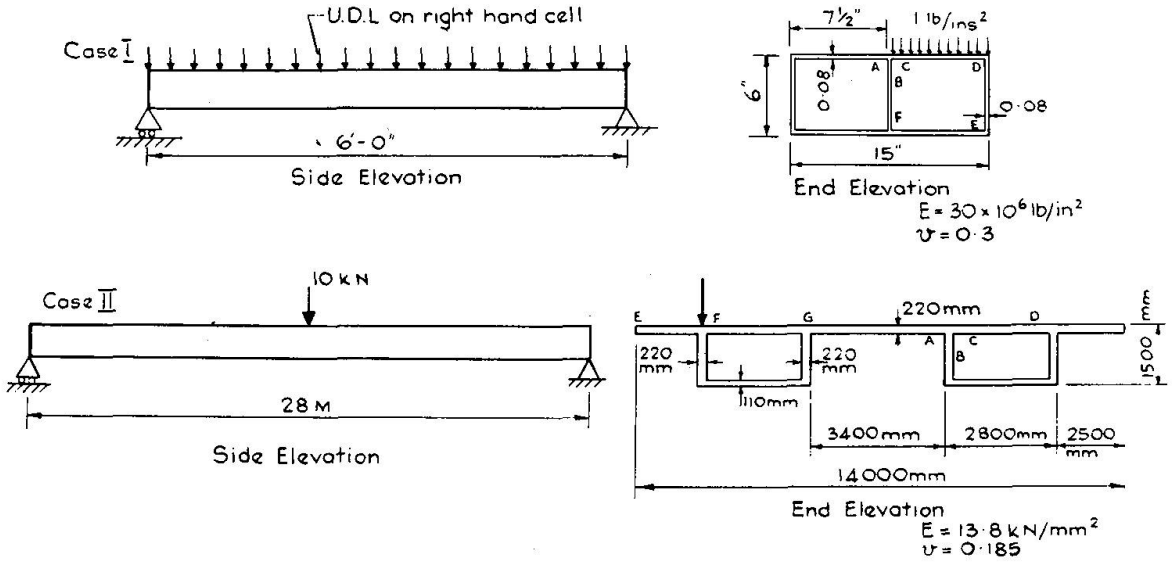

Fig. 19. Typical sections considered.

In Fig. 19, Case I shows a simply supported double-cell steel box, the girder being subjected to a transversely unsymmetrical loading consisting of a uniformly distributed load applied over one of the cells. Certain, typical results for this girder are listed in Table 1 – Case I and it is seen that the values of transverse moments, longitudinal stresses and deflections given by the Nodal Section Method agree closely with those given by the Folded Plate Method.

Similarly, close agreement of the values given in Table 1 – Case II is observed, these values having been obtained for the typical discreet-cell, concrete girder illustrated in Fig. 19 Case II. The convergence characteristics of the Nodal Section solution for this girder have been discussed earlier and shown in Fig. 12b and the results given in Table 1 – Case II were obtained after the third iterative cycle. For a point loading applied over a web, such as that shown in Fig. 19 – Case II, the Nodal Section Method, in common with most other methods, is not capable of predicting accurate values of the extremely high stresses set up in the immediate vicinity of the point loads. However, at positions away from the point load, satisfactory values are given by the method, as shown in the table.

Table 1. Case I – Double-cell girder

Solution	Transverse Moms (lbs ins/inch) at ½ – span				Longit. stresses (lbs/ins^2) at 2/5 – span				Deflections (ins × 10^{-5}) at ½ – span			
									Vert.		Horiz.	
	Pt.A	Pt.B	Pt.C	Pt.D	Pt.B	Pt.D	Pt.E	Pt.F	Pt.B	Pt.D	Pt.B	Pt.F
Folded Plate	1.27	−3.17	4.44	2.39	558	1129	−1130	−556	39.5	745	145	−145
Nodal Section	1.37	−3.08	4.44	2.41	534	1135	−1135	−534	33.1	705	149	−149

Case II – Discreet-cell girder

Solution	Transverse Moms (Nmm/mm) at ½ – span				Longit. stresses (N/mm^2 × 10^4) at 2/5 – span				Vert. deflection (mm × 10^3) at ½ – span			
	Pt.A	Pt.B	Pt.C	Pt.D	Pt.E	Pt.F	Pt.G	Pt.A	Pt.F	Pt.G	Pt.B	
Folded Plate	403	304	99	6.2	206	200	167	130	432	343	196	
Nodal Section	474	361	113	7.5	206	186	161	130	352	330	210	

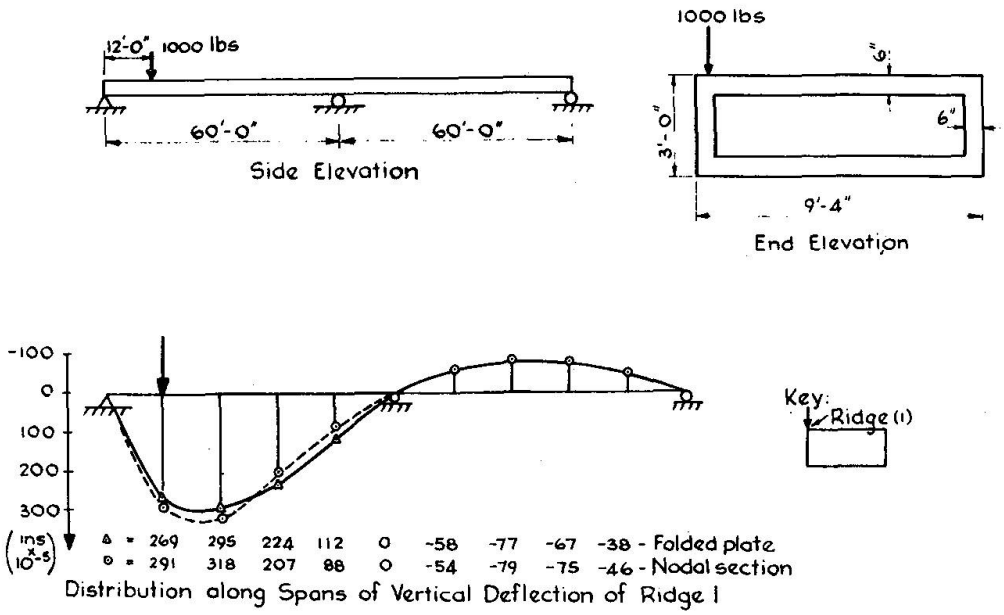

Fig. 20. Results for unsymmetrically loaded continuous girder.

All the girders considered in the comparison so far have been simply supported, but in Fig. 20 a continuous single-cell girder subjected to an unsymmetrical point loading over one web is illustrated, the loading being applied to one span only at a position close to the end support. In the figure, the variation along both spans of the vertical deflection of the loaded joint is plotted, and the unsymmetrical nature of the behaviour about the mid-span support position is clearly illustrated. The curves predicted by both the Nodal Section and Folded Plate methods are seen to correspond closely in both the loaded and unloaded spans.

Finally, the tapered girder shown in Fig. 21 was analysed, the girder once again being subjected to an unsymmetrical line loading applied over one of the webs. In this case, the Folded Plate method could not be used in the analysis since it is not capable of dealing with girders of non-uniform cross-section, consequently, the Nodal Section results are compared to values obtained by the Finite Element Method. In the figure, the variation along the span of the vertical deflection of a typical joint is plotted together with the distribution of the transverse moments and longitudinal stresses around the mid-span cross-section, and the Nodal Section and Finite Element values are once again seen to agree closely in all cases.

6. Advantages of the Nodal Section Method

The nodal section method provides a simple and accurate method of analysis for box girders. The computer programme (BOXGDR) based on the method requires relatively little computer time and storage space and is thus an economical means of analysing girders at the design stage, when many analyses may be necessary in order to achieve the optimum dimensions. The programme has the further advantage that both the preparation of data and the interpretation of results is relatively simple thus leading to additional significant economies.

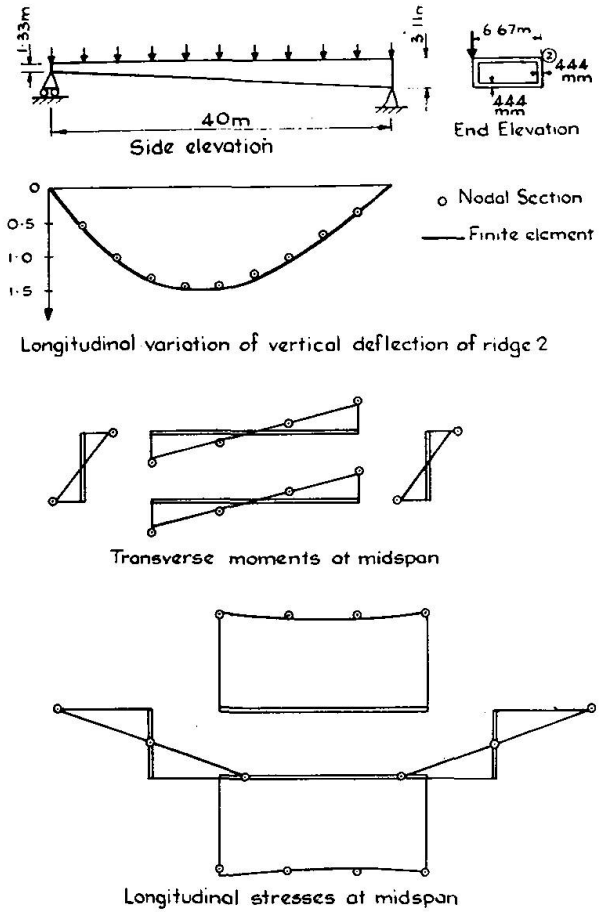

Fig. 21. Results for tapered girder.

Furthermore, the sequential nature of the calculations enables solutions to be obtained by hand, in many cases, without requiring the use of digital computers. In addition to the obvious economic advantages, such a hand solution enables the engineer to retain a better appreciation of the structural behaviour, particularly since each step within the analysis is related to a certain aspect of the physical behaviour.

Finally, the nodal section method is extremely adaptable and may be applied to the analysis of box girders of any cross-sectional shape under any loading conditions. It is also the only method, other than the very expensive finite element method, that is capable of dealing with the analysis of box girders in which the geometry of the cross-section varies along the span. Such girders are, of course, frequently encountered in practice, as, for example, in the case of motorway bridges having web plates of varying depths.

7. Conclusions

In this paper, the basic theory of the Nodal Section Method has been presented and the accuracy of the method in the analysis of a number of different girders has been illustrated. It is anticipated that this accuracy, coupled with the simplicity of the solution procedure, which enables solutions to be obtained either by

hand or from a computer programme that is very economical of computer time and storage space, will make the method a valuable analytical tool for use during the design of box girders.

Several developments of the method are in hand at the present time. In the first place, the method is being extended to consider the effects of shear lag on the distribution of the longitudinal stresses set up in the flanges of a girder, and the proposed approach (13), which is based on the use of empirical factors, has yielded results of good accuracy. The method is also being developed for the analysis of box girders curved in plan, and results obtained to date show excellent agreement between the Nodal Section values and values obtained both experimentally and from a Finite Element study. Finally, the analysis of girders on skew supports and girders containing deflecting internal diaphragms is being considered together with the behaviour of girders of non-uniform cross-section. All these developments will greatly extend the field of application of the method without, in any way, affecting the simplicity and economy of the solution procedure.

The integration of the Nodal Section Method with a Finite Element solution is also being considered. Such an arrangement has been described in the present paper in the method for dealing with concentrated loadings. It is intended to develop this technique further so that the designer can if he wishes, when dealing with a position of rapidly changing stress, such as at column supports and internal diaphragms, use a Finite Element Solution to provide a more detailed picture of the stress field in the local area. This procedure thus providing an accurate and economical method of analysis with great adaptability and a wide field of application.

List of Symbols

$1... n... n_o$	nodal section numbering.
$1... p... p_o$	plate numbering.
$1... j... j_o$	joint numbering.
A and B	plate edge labels.
AD	connectivity matrix.
S	plate width.
t	plate thickness.
$\varnothing$	inclination of plate to horizontal.
M	transverse bending moments.
N	longitudinal shear forces at the edges of the plate beams.
σ	longitudinal stresses.
Δ	sway displacement of a plate.

Acknowledgments

The Authors wish to thank the Highways Engineering Computing Branch of the Department of the Environment and R. Travers Morgan & Partners, Consulting Engineers, for sponsoring the development of the Nodal Section Method.

In particular, the Authors gratefully acknowledge the many fruitful discussions that they have had with Dr. R.G. Anderson of R. Travers Morgan & Partners.

The Authors are also indebted to Mr. J.W. Waddell, postgraduate student at the Department of Civil and Structural Engineering, University College, Cardiff, for the assistance that he has given in many stages of the investigation.

References

1. GOLDBERG, J.E., and LEVE, H.L.: Theory of Prismatic Folded Plate Structures. Publs. int. Ass. Bridge Struct. Engng, Vol. 17, 1957, pp. 59–86.
2. DE FRIES SKENE, A., and SCORDELIS, A.C.: Direct Stiffness Solution for Folded Plates, J. Struct. Div. Am. Soc. Civ. Engrs., Vol. 90, ST4, August 1964, pp. 15–47.
3. GAAFAR, I.: Hipped Plate Analysis, Considering Joint Displacements. Trans. Am. Soc. Civ. Engrs., Vol. 119, 1954, pp. 743–784.
4. YITZHAKI, D.: The Design of Prismatic and Cylindrical Shell Roofs. Haifa, Haifa Science Publishers, 1958.
5. SCORDELIS, A.C.: Analysis of Simply Supported Box Girder Bridges. University of California, Berkeley, Report No. SESM 66-17, October 1966.
6. SCORDELIS, A.C.: Analysis of Continuous Box Girder Bridges. University of California, Berkeley, Report No. SESM 67-25, November 1967.
7. EVANS, H.R., and ROCKEY, K.C.: A Critical Review of the Method of Analysis for Folded Plate Structures, Proc. Instn. Civ. Engrs., 1971, 49 (June), pp. 171–192.
8. ROCKEY, K.C., and EVANS, H.R.: A Hand Solution Technique for Box Girders. To be published.
9. JOHNSON, C.D., and LEE, T.: Long Nonprismatic Folded Plate Structures, J. Struct. Div. Am. Soc. Civ. Engrs., Vol. 49, ST6, June 1968, pp. 1457–1484.
10. PUCHER, A.: Influence Surface of Elastic Plates. Springer Verlag, Vienna, New York, 1964.
11. ROCKEY, K.C., and EVANS, H.R.: A Report on the Nodal Section Method. University College, Cardiff, Report No. NS/C/9, November 1972.
12. MAST, P.E.: An Iteration Method for Folded Plate Analysis. Proc. World Conference on Shell Structures, 1962, National Academy of Sciences, Washington D.C., 1964, pp. 517–526.
13. ROCKEY, K.C., and EVANS, H.R.: The Development of the Nodal Section Method to Include the Effects of Shear Lag. University College, Cardiff, Report No. NS/C/Extra 2, June 1974.
14. ROCKEY, K.C., and EVANS, H.R.: An Assessment of the Accuracy of the Nodal Section Method. University College, Cardiff, Report No. NS/Par/1, March 1974.

Summary

This paper describes the basic theory of the Nodal Section Method. This method has been developed for the analysis of box girders and, by assuming an idealised structural behaviour, it provides a simplified solution procedure, which it is anticipated will prove to be of use during the design stage, when many analyses of the girder may be required. Results are presented for many different types of box girders, the values given by the Nodal Section Method being compared to those obtained from other established methods, and the accuracy of the Nodal Section values is illustrated.

Résumé

La contribution décrit la théorie de base de la méthode de section nodale. Cette méthode a été développée pour l'analyse de poutres en caisson et, en admettant un comportement structural idéalisé, elle fournit une solution de procédure simplifiée, laquelle s'avère utile durant la phase du projet lorsque beaucoup d'analyses de poutres sont demandées. On présente des résultats pour de nombreux types différents de poutres en caisson; les valeurs fournies par la méthode de section nodale sont comparées à celles obtenues par d'autres méthodes établies. La précision des valeurs de la section nodale est démontrée.

Zusammenfassung

Die vorliegende Arbeit beschreibt die Grundtheorie der nodalen Querschnitts-Methode. Diese wurde zur Berechnung von Brückenträgern entwickelt; unter Annahme eines idealisierten baulichen Verhaltens liefert sie eine vereinfachte Verfahrenslösung, welche sich während des Projektstadiums als nützlich erweist, falls viele Berechnungen für den Träger erforderlich sind. Es werden Resultate für zahlreiche Typen von Kastenträgern mitgeteilt, wobei die aus der nodalen Querschnitts-Methode herrührenden Werte mit jenen von anderen Methoden verglichen werden und die Genauigkeit der nodalen Querschnittswerte veranschaulicht wird.